

# Banding Artifact Reduction in Electrophotographic Processes Using OPC Drum Velocity Control

*Cheng-Lun Chen<sup>1</sup>, George T.-C. Chiu<sup>1</sup> and Jan P. Allebach<sup>2</sup>*

*<sup>1</sup>School of Mechanical Engineering,*

*<sup>2</sup>School of Electrical and Computer Engineering*

*Purdue University*

*West Lafayette, Indiana*

## Abstract

This paper proposed a new process control strategy for reducing banding artifacts in electrophotographic (EP) processes. EP banding artifact is shown to correlate to the fluctuation of the organic photoconductive (OPC) drum angular velocity. Improved regulation of the OPC drum rotational velocity under various process uncertainty and variations will significantly improve EP process stability and reduce the appearance of banding. The proposed control strategy includes two levels of OPC drum speed regulation. The first level utilizes a loop shaping technique to incorporate a human visual system (HVS) model into the control loop to eliminate low frequency and non-periodic drum velocity fluctuation. The second level uses an internal model based repetitive controller to reduce the effect of periodic velocity fluctuations. The HVS based loop shaping design is intended to address the subjective evaluation of printing process by incorporating human visual perception into EP process control. Experimental verification on a typical low cost 600-dpi EP engine showed significant banding reduction for spatial frequency up to 70 cycles per inch.

## Introduction

Electrophotography (EP) is the basic imaging process used in paper copiers and laser printers. For typical EP process, the image quality strongly depends on the six basic steps, i.e. charging, exposure, developing, transferring, fusing, and cleaning. Thus, any factor affecting those above processes would definitely affect the image quality. Wulich and Kopeika<sup>1</sup> pointed out that mechanical vibration would limit the resolution of an EP process. Kawamoto showed that electrostatic force on charge roller and cleaner blade chattering are two such vibration sources.<sup>2,3</sup> Schubert studied periodic image artifact resulting from wobbling of the rotating polygon mirror.<sup>4</sup> Among various well-known image artifacts, halftone banding due to scan line spacing variation

is one of the most visible defects, which appears as light and dark streaks across a printed page perpendicular to the process direction.

Some literature has been devoted to the modeling and analysis of banding in EP process. Burns et al. discovered that laser beam positioning error would result in undesirable image noise, which degrades the image quality.<sup>5</sup> Melnychuck et al. identified strong correlation between the scan line spacing variation and the occurrence of banding.<sup>6</sup> Loce et al. modeled vibration-induced halftone banding in laser printers.<sup>7</sup> Although scan line spacing and reflectance variation are shown to be direct contributor of banding, a model of the human visual system is needed to reflect the actual banding perceived by human eyes. The contrast sensitivity function (CSF) is one of such models that help capturing the modulation transfer function (MTF) of human eyes on perceiving spatial information. Several researches have contributed to the analysis and synthesis of CSF function, which has been used by other researchers to quantify perceived image quality.<sup>8,9</sup> The bandpass-like CSF function reveals the fact that mid-frequency disturbances have greater impact on perceived banding so that a banding cancellation scheme should supply its reduction effort mainly on bandings located in this frequency region.

Different approaches for banding reduction have been addressed recently.<sup>10-19</sup> The first approach<sup>10,11,12</sup> is to design better gear train, i.e. gear meshing or gear pitch, to either reduce transmission error or push the vibration into high frequency region. The second approach<sup>13,14,15</sup> is to deflect the laser beam in the process direction to compensate for the line spacing variation. The third approach<sup>16-19</sup> is to modulate the laser power to directly compensate for the absorptance variation due to line spacing error. However, little has been documented in the attenuation or cancellation of drum speed perturbation due to undesirable excitations using closed-loop feedback control approaches. An advantage, often neglected by researchers, of using feedback control is its ability to withstand system uncertainties (e.g. component replacing and aging) in practical situation, which cannot be

tackled by simply increasing manufacturing precision. On the other hand, the velocity regulation of the OPC drum is more of a challenge since the main drive motor transmits the power to the OPC drum through the gear train that is also responsible for driving all the other loading, i.e. auxiliary rollers and transporting the paper. Typical motor velocity regulation scheme has been shown to have limitation on attenuating the velocity fluctuation on the OPC drum.<sup>20</sup>

Since the majority of the OPC drum velocity variation is of known and constant periods that are related to the transmission gearing, repetitive control is a feasible solution to compensate for these periodic disturbances. Repetitive control based systems have been shown to work well for tracking periodic reference commands and rejecting periodic disturbances in regulation applications. The analysis and synthesis of repetitive controllers for continuous-time single-input-single-output (SISO) systems were first proposed by Hara et al. and they extended the idea to MIMO systems in 1988.<sup>21</sup> Almost at the same time, Tomizuka et al. addressed the analysis and synthesis of discrete-time repetitive controller considering the fact that digital implementation of a repetitive controller is simpler and doesn't require the controlled plant to be proper.<sup>22</sup>

In this paper, a two level closed-loop OPC drum velocity regulation control is proposed to improve the EP process stability by reduce the sensitivity of the OPC drum velocity regulation to both periodic and non-periodic disturbances and manufacturing uncertainties. Unlike typical low-cost laser printers, the proposed OPC drum velocity loop is closed at the OPC drum angular position through an optical encoder. To account for the effect of the human visual system in interpreting non-periodic and low spatial frequency artifacts, a human visual system (HSV) based loop shaping controller is design to incorporate the human CSF into the primary loop design. The HVS based controller also helps to eliminate DC drifts as well as provide robustness to the OPC drum velocity control loop. A second level repetitive controller is then design to compensate for the periodic disturbances that are the major contributors to EP banding. With the removal of the DC components of the disturbances by HSV based controller, the nominal (mean) value of the OPC drum angular velocity is constant. Thus, the fundamental and harmonic frequencies of the periodic disturbances will be stationary and the repetitive control algorithm can be applied directly without modification. The effectiveness of the proposed control system is verified by applying it to a typical 600 dpi EP engine. Experimental results shown significant disturbance reduction in scan line spacing within the spatial frequency range (< 70 cycles/inch) where HVS is most sensitive to periodic artifacts. Actual printout shows significant visual improvement in banding.

## System Description

### The EP Printing System

The imaging part of an EP printing system or laser

printer can be viewed as the combination of two subsystems as shown in Figure 1. The first subsystem is composed of the main drive brushless DC (BLDC) motor with its onboard driver, the gear trains and the OPC drum. Its main task is to supply torque to preserve constant angular velocity of the OPC drum. The driver controls the velocity of the motor by adjusting the amount of currents flowing through the armature windings of the motor. The motor shaft drives the gear train that connects with the OPC drum. The gear train is a couple of gears that serve the purpose of obtaining the required velocity reduction from the motor to the OPC drum. Phase locked loop (PLL) and pulse width modulation (PWM) are two of the most popular methods utilized in marketed BLDC drivers for achieving the desired velocity regulation. The second subsystem is basically the optics, the laser control unit, the laser diode and the polygon mirror that deflects the laser beam to the OPC drum. Its task is to control the intensity and location of the laser. The laser control unit generates pulses which control the on-off of the laser diode according to the image that is to be exposed on the OPC drum. In this paper, we will focus on the control of the first subsystem. The strategy here is to use the angular position of the OPC drum to control the drive signal input to the BLDC motor, thereby stabilizing the OPC drum velocity. Since the motor rotates at a much higher velocity than the OPC drum, high-resolution control of the OPC drum velocity is possible. A typical 600 dpi EP engine is used. A high-resolution optical encoder capable of 50,000 pulses per revolution is mounted on the OPC drum. Thus, a closed loop control system is formed, which includes the BLDC motor, the gear train in between, and the OPC drum.

### Effect of OPC Drum Velocity on Print Quality

Although it has been shown that OPC drum velocity fluctuation would cause scan line spacing variation<sup>7</sup>, a more rigorous relation between the line spacing and the OPC drum velocity can be derived by inspecting Figure 2, where  $f_s$  is the laser beam scanning frequency,  $\Delta l$  is the line spacing,  $r$  is the radius of rotation, and  $\theta$  and  $w$  are drum rotating angle and rotating velocity, respectively. A fundamental equation based on geometry can be found to be

$$dl = \sqrt{(dr)^2 + (rd\theta)^2} \quad (1)$$

so that

$$\frac{dl}{d\theta} = \sqrt{\left(\frac{dr}{d\theta}\right)^2 + r^2} \quad (2)$$

or

$$\frac{dl/dt}{d\theta/dt} = \sqrt{\left(\frac{dr}{d\theta}\right)^2 + r^2} \quad (3)$$

Use the fact that  $w = d\theta/dt$ , we have

$$\frac{dl}{dt} = w \sqrt{\left(\frac{dr}{d\theta}\right)^2 + r^2} \quad (4)$$

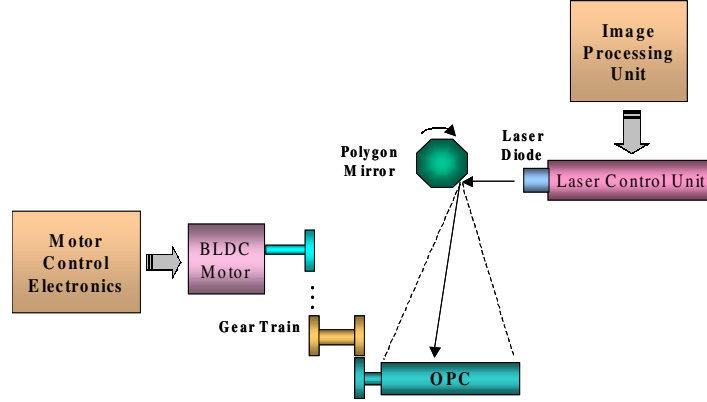


Figure 1. Diagram of the EP printing system.

Now suppose that  $(l_0, t_0)$  is the coordinate pair representing the measured linear displacement at time  $t_0$ . The line spacing thus is given by the following equation.

$$\Delta l = \int_{l_0}^{l_0 + \Delta l} dl = \int_{t_0}^{t_0 + 1/f_s} w \sqrt{\left(\frac{dr}{d\theta}\right)^2 + r^2} dt \quad (5)$$

Note that no assumptions like constant velocity or rotating radius and constant scanning frequency are made here, so the above equation provides more general kinematical relationship among those variables.

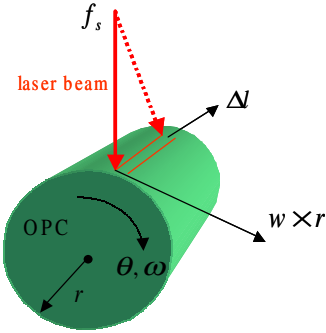


Figure 2. Relationship among scan line spacing, radius of rotation, and OPC drum velocity.

To investigate only the effect of drum velocity variation on line spacing, the scanning frequency  $f_s$  and the radius of rotation  $r$  are assumed to be constant. Although it has been known that most of the velocity disturbances in the EP process are inherently periodic, it is safe to take only the fundamental frequency, which is sinusoidal, for analysis since magnitudes of other high-frequency harmonics are usually much smaller. Suppose that the nominal or desired OPC drum velocity  $w_0$  (rad/s) has variation with magnitude

$d$  (rad/s), frequency  $f_d$  (Hz), and phase  $\phi$  (radians) such that

$$w = w_0 + d \sin(2\pi f_d t + \phi) \quad (6)$$

Substituting Eq. (6) into Eq. (5) yields

$$\Delta l = r_0 \int_{t_0}^{t_0 + 1/f_s} [w_0 + d \sin(2\pi f_d t + \phi)] dt \quad (7)$$

$$\begin{aligned} &= \frac{w_0 r_0}{f_s} + \frac{dr_0}{\pi f_d} \sin\left(2\pi f_d t_0 + \phi + \pi \frac{f_d}{f_s}\right) \sin\left(\pi \frac{f_d}{f_s}\right) \\ &= \frac{w_0 r_0}{f_s} + \frac{dr_0}{f_s} \sin\left(\pi \frac{f_d}{f_s}\right) \sin\left(2\pi f_d t_0 + \phi + \pi \frac{f_d}{f_s}\right) \end{aligned}$$

Several interesting points can be drawn from Eq. (7):

1. When the nominal or desired line spacing is  $\Delta l_0 = w_0 r_0 / f_s$ , the maximum line spacing fluctuation is given by

$$\max_t (\Delta l - \Delta l_0) = \frac{dr_0}{f_s} \sin\left(\pi \frac{f_d}{f_s}\right) \quad (8)$$

2. The velocity variation induces line spacing variation with the same frequency.
3. The maximum line spacing fluctuation rate due to OPC drum velocity variation can be defined as

$$\frac{\Delta l - \Delta l_0}{\Delta l_0} = \frac{dr_0 / f_s}{w_0 r_0 / f_s} \sin\left(\pi \frac{f_d}{f_s}\right) = \frac{d}{w_0} \sin\left(\pi \frac{f_d}{f_s}\right) \quad (9)$$

It is quite obvious to see that maximum line spacing error is proportional to maximum velocity variation. Figure 3 shows how amounts of OPC drum velocity variation and frequencies affect the maximum line spacing fluctuation when the scanning line frequency is fixed at 1 kHz. It can be seen that with same magnitude of velocity fluctuation, low frequency disturbances tend to induce larger line spacing error.

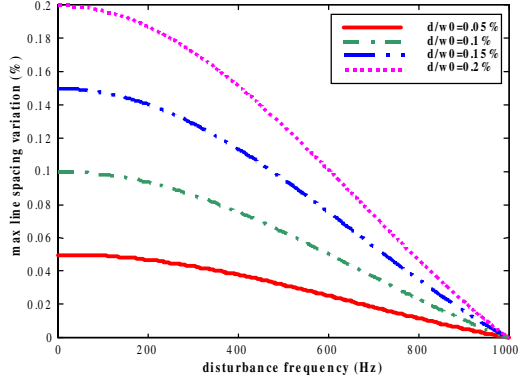


Figure 3. Effect of magnitude and frequency of velocity fluctuation on maximum line spacing error.

### Controller Design

#### Closed-Loop OPC Drum Velocity Regulation

A schematic of the proposed closed loop system is depicted in Figure 4. Two separate controllers are to be designed based on the transfer function from  $e(s)$  to  $u(s)$ , which is the so-called plant. A 3rd order model is fitted to the experimental frequency response of the plant as having the following transfer function.

$$G_0(s) = \frac{2.046 \times 10^7}{s^3 + 801.3 s^2 + 4.443 \times 10^5 s + 4.326 \times 10^6} \quad (10)$$

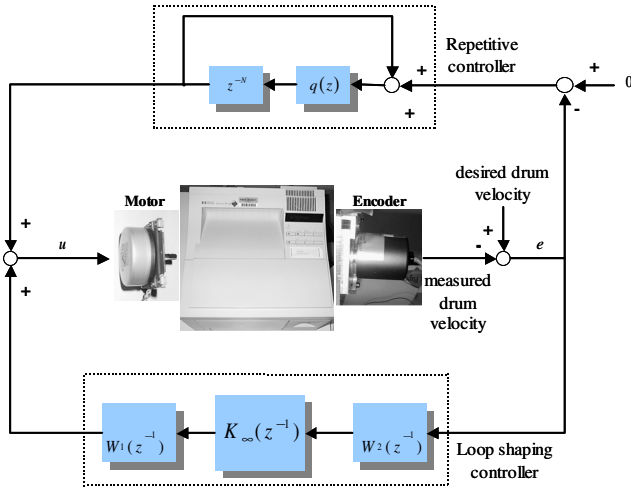


Figure 4. Configuration of the closed loop control system.

The loop-shaping controller forms the first layer control, which will reject those non-periodic disturbances lying within the low frequency region. Note that this layer of control also aims at eliminating the dc component of the

disturbances so that the frequencies of the remaining periodic components will be fixed. The repetitive controller then forms the second layer of control to cancel those periodic disturbances. The input to the controllers,  $e(s)$ , is the angular velocity error of the OPC drum measured by an optical encoder and the control effort  $u(s)$  to the motor driver are summation of the computed outputs from both controllers.

#### Synthesis of the HVS $H_\infty$ Loop Shaping Controller

The guideline for  $H_\infty$  loop shaping design is available in existing literature. (e.g. Zhou's book) The objective is to design feedback controllers such that the open-loop transfer function has high gain at the specific frequencies where disturbances are to be rejected. The CSF is a good target for shaping the open loop transfer function gain where high gain is required to reduce the effect of banding (high contrast sensitivity values). It also provides a guideline for reducing the open-loop transfer function gain to provide robustness for actuator bandwidth limitation and model uncertainty (low contrast sensitivity). There are various versions of CSF functions in the existing literature, see Figure 5. For low-order filter design, Barten modified Mannos' CSF to have low pass characteristic. That is

$$CSF(f_1) = a \times (b + cf_1) e^{\{-(cf_1)^d\}}, \text{ if } f_1 \geq f_{\max} \quad (11)$$

$$CSF(f_1) = a \times (b + cf_{\max}) e^{\{-(cf_{\max})^d\}}, \text{ if } f_1 < f_{\max}$$

with  $a=2.6$ ,  $b=0.0192$ ,  $c=0.114$ ,  $d=1.1$ , and

$$f_1 = \frac{f \times \pi}{360 \times \tan^{-1}(1/2v_d)} \quad (12)$$

where  $v_d$  is the viewing distance in inch,  $f$  is the spatial frequency in cycles/in, and  $f_1$  is in cycles/deg. Note that  $f_{\max}$  satisfies the following equation:

$$1 - bc^{d-1} df_{\max}^{d-1} - c^d df_{\max}^d = 0 \quad (13)$$

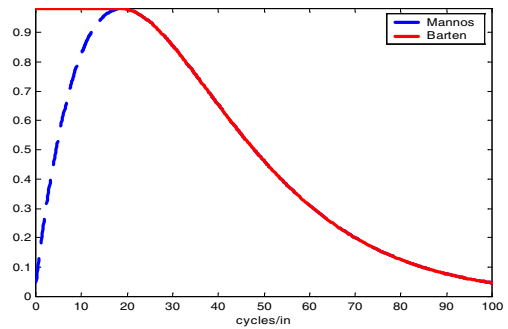


Figure 5. CSF's at viewing distance of 24".

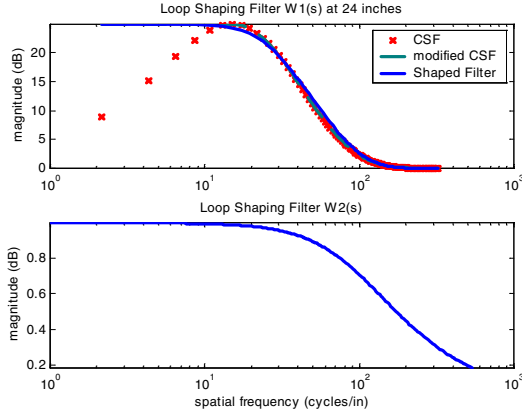


Figure 6. Frequency responses of the weighting filters.

From feedback control design point of view, a certain amount of low frequency gain is needed to maintain an acceptable steady state regulation performance. Hence, Barten's modified CSF would be a better interpretation of the desired frequency dependent magnitude profile of the open-loop transfer function of the OPC drum velocity control system. A  $H_\infty$  loop shaping approach will be employed to design a suitable controller for the first layer control. The pre-compensator  $W_1$  (for performance) and post-compensator  $W_2$  (for stability robustness) are properly chosen to shape the loop transfer function of the augmented plant  $W_2GW_1$  into the desired one, see Figure 4.  $K_\infty$  is then found by the existing searching algorithm. The feedback controller is then formed by  $K = W_1K_\infty W_2$ . Here  $W_1$  is chosen to be a stable and minimum phase filter that approximates the above-mentioned CSF with the viewing distance of 24 inch, while  $W_2$  is chosen as a strictly proper filter that rolls off the controller at high frequency. Besides, both are chosen to be low order filters to avoid producing high order controller. After several iterations, two acceptable filters are selected as

$$W_1(s) = \frac{s^2 + 1579s + 1.374 \times 10^6}{s^2 + 392.4s + 7.757 \times 10^4} \quad (14)$$

$$W_2(s) = \frac{1}{0.0008595s + 1} \quad (15)$$

Figure 6 shows the frequency responses of the two filters. The searching algorithm gives us an 8th order stabilizing compensator:

$$K(s) = -\frac{3817s^7 + 1.35 \times 10^7 s^6 + 2.28 \times 10^{10} s^5}{s^8 + 428s^7 + 8.07 \times 10^6 s^6 + 9.26 \times 10^9 s^5} + \frac{2.25 \times 10^{13} s^4 + 1.38 \times 10^{16} s^3 + 5.94 \times 10^{18} s^2}{+7.34 \times 10^{12} s^4 + 4.06 \times 10^{15} s^3 + 1.49 \times 10^{18} s^2} + \frac{1.42 \times 10^{21} s + 1.70 \times 10^{23}}{+3.11 \times 10^{20} s + 3.28 \times 10^{22}} \quad (16)$$

## Synthesis of the Repetitive Controller

To synthesis that is capable of rejecting a periodic disturbance (i.e. a sinusoidal component and all its harmonics), consider the closed loop system  $G_c$  representing the transfer function from the controller input to the velocity error output after plugging in the loop-shaping controller:

$$G_c(z) = z^{-d} B(z^{-1}) / A(z^{-1}) = z^{-d} B^+ B^- / A(z^{-1}) \quad (17)$$

where  $d$  is the number of delay steps in the system.  $B^+(z^{-1})$  and  $B^-(z^{-1})$  are parts of  $B(z^{-1})$  with the cancelable and uncancelable zeros, respectively. It is known that the prototype repetitive controller  $G_r$  can be synthesized as

$$G_r(z) = k_r R(z^{-1}) / S(z^{-1}) \frac{z^{-N}}{1 - z^{-N}} \quad (18)$$

with

$$R(z^{-1}) = k_r z^d A(z^{-1}) B^-(z),$$

$$S(z^{-1}) = B^+(z^{-1}) b, \quad b \geq \max |B^-(e^{-jw})|^2, \quad w \in [0, \pi].$$

Note that  $0 < k_r < 2$  and  $N = f_s / f_d$ , where  $f_s$  is the sampling frequency of the discrete-time system and  $f_d$  is the fundamental frequency of disturbances to be rejected. A zero-phase error low pass filter  $a(z) = (z^{-1} + a + z) / (a + 2)$  with  $a \in \mathbb{Z}^+$  is usually introduced in the forward or feedback loop of the delay taps to improve stability robustness.

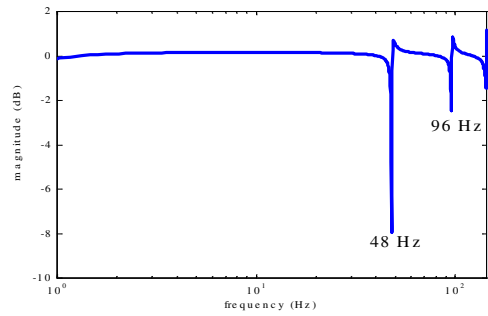


Figure 7. Frequency response of the HVS/repetitive control system showing its capability of rejecting the periodic disturbance with fundamental frequency of 48 Hz.

## Experimental Results

The proposed control scheme is applied to a typical 600 dpi EP engine. The encoder resolution is set to 50,000 pulses/rev with 2-bit interpolation. The sampling frequency of the experimental system is set to 1200 Hz. The fundamental frequency of the disturbance after closing the loop using the HVS based controller is 48 Hz (which is about 25.8 cycles/in), so the period of the repetitive controller  $N$  is set to 25. The capability of the system for rejecting the disturbance at 48 Hz and its harmonics after

plugging in the repetitive controller is depicted in Figure 7. In the experiment, the repetitive controller is turned on after the loop-shaping controller is activated. Figure 8 shows the comparison of the disturbance spectrum among the experiments before compensation, with the loop-shaping controller, and with the loop shaping plus the repetitive controller. It can be seen that the repetitive controller has significantly reduced the disturbance at 48 Hz. Figure 9 shows the printed images of the uncompensated and the compensated system. There is significant print quality improvement after implementing the controller combining the HVS based loop shaping and the repetitive control.

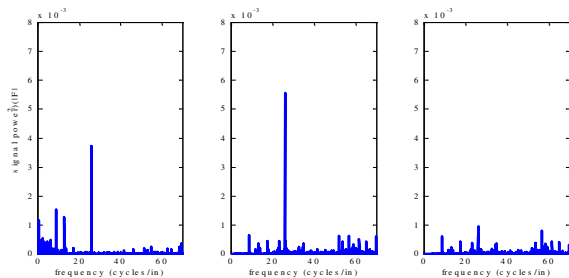


Figure 8. Experimental results before compensation (left), with HVS loop shaping (middle), and with HVS/repetitive control (right).



Figure 9. Actual printouts before (top) and after compensation (bottom).

## Conclusions

In this paper, a new feedback architecture and control scheme for EP process is presented to effectively reduce banding artifacts. The proposed control structure combines a HVS based loop-shaping controller with a repetitive controller. The feasibility and effectiveness of the new control strategy is experimentally verified. Although a high-resolution encoder is used here, the new control configuration is verified to also work well with low-resolution analog encoder when suitable hardware interpolation is incorporated.

## References

1. D. Wulich and N. S. Kopeika, Image resolution limits resulting from mechanical vibrations, *Optical Engineering*, **26**, no. 6, pp. 529-533 (1987).
2. H. Kawamoto, K. Udagawa, and M. Mori, Vibration and noise induced by electrostatic force on a contact charger roller of electrophotography, *Journal of Imaging Science and Technology*, **39**, no. 6, pp. 477-480 (1995).
3. H. Kawamoto, Chatter vibration of a cleaner blade in electrophotography, *Journal of Imaging Science and Technology*, **40**, no. 1, pp. 8-13 (1996).
4. P. C. Schubert, Periodic image artifacts from continuous-tone laser scanners, *Applied Optics*, **25**, no. 21, pp. 3880-3884, (1986).
5. P.D. Burns, M. Rabbani, and L.A. Ray, Analysis of image noise due to position errors in laser writers, *Applied Optics*, **25**, no. 13, pp. 2158-2168 (1986).
6. P. Melnychuck and R. Shaw, Fourier spectra of digital halftone images containing dot position errors, *Journal Optical Society of America*, **5**, no. 8, pp. 1328-1338 (1988).
7. R. P. Loce, W. L. Lama, and M. S. Maltz, Modeling vibration-induced halftone banding in a xerographic laser printer, *Journal of Electronic Imaging*, **4**, no. 1, pp. 48-61 (1995).
8. J. L. Mannos and D. J. Sakrison, The effects of a visual fidelity criterion on the encoding of images, *IEEE Trans on Information Theory*, **IT-20**, no. 4, pp. (1974).
9. P. Barten, Evaluation of subjective image quality with the square-root integral method, *J. Opt. Soc. Am*, **7**, no. 10, pp. (1990).
10. Y. Hotta, M. Goto, and T. Miyamoto, Image forming apparatus having relationship between driving gear pitch and scanning line pitch, U.S. Patent 5,917,529 (1999).
11. P. L. Jeran, Gear train control system for reducing velocity induced image defects in printers and copiers, U.S. Patent 5,812,183 (1998).
12. T. Kusuda, M. Ikeda, T. Ogiri, and T. Besshi, Transmission deviation caused by eccentricity in multi gear systems, *PICS: Image Processing, Image Quality, Image Capture, Systems Conference*, Savannah, Georgia, 1999, pp. 119-124.
13. R. J. Lawton and D. R. Marshall, Beam deflecting for resolution enhancement and banding reduction in a laser printer, U.S. Patent 5,920,336 (1999).
14. W. E. Foote and R. G. Sevier, Laser printer with apparatus to

- reduce banding by servo adjustment of a scanned laser beam, U.S. Patent 5,760,817 (1998).
15. K. Bannai, Image forming apparatus with anti-banding implementation, U.S. Patent 5,315,322 (1994).
  16. R. P. Loce and W. L. Lama, Printer compensated for vibration-generated scan line errors, U.S. Patent 4,884,083 (1989).
  17. D. W. Costanza, R. E. Jodoin, and R. P. Loce, Method and apparatus for compensating for raster position errors in output scanners, U.S. Patent 5,900,901 (1999).
  18. R. D. Morrison, System and method for modifying an output image signal to compensate for drum velocity variations in a laser printer, U.S. Patent 5,729,277 (1998).
  19. W. L. Lama, R. P. Loce, and J. A. Durbin, Image bar printer compensated for vibration-generated scan line errors, U.S. Patent 4,801,978 (1989).
  20. C.-L. Chen and G. T.-C. Chiu, Banding Reduction in Electrophotographic Process, *IEEE/ASME International Conference of Advanced Intelligent Mechatronics*, Como, Italy, 2001, pp. 81-86.
  21. S. Hara, Y. Yamamoto, T. Omata, and M. Nakano, Repetitive control system: A new type servo system for periodic exogenous signals, *IEEE Trans. Automatic Control*, **33**, no. 7, pp. 659-668 (1988).
  22. M. Tomizuka, T. C. Tsao, and K. K. Chew, Analysis and synthesis of discrete-time repetitive controllers, *ASME J. Dynamic Systems, Measurements and Control*, **111**, no. 3, pp. 353-358 (1989).
  23. K. Zhou and J. Doyle, *Essentials of Robust Control*, Prentice Hall, 1997.

### Biography

Cheng-Lun Chen received his BS and MS degrees from National Tsing-Hua University, Taiwan (Department of Power Mechanical Engineering) in 1993 and 1995, respectively. His MS thesis is on torque ripple analysis of axial-field miniature BLDC motor. Since 1998 he has been studying towards his Ph.D degree in the School of Mechanical Engineering, Purdue University at West Lafayette. His current research interest focuses on modeling, disturbance source identification, closed-loop control and banding characterization of EP process.